

Role of Orbital Degeneracy in Double Exchange Systems

M. S. Laad¹, L. Craco² and E. Müller-Hartmann¹

¹*Institut für Theoretische Physik, Universität zu Köln, 77 Zùlpicher Strasse, D-50937 Köln, Germany*

²*Instituto de Física Gleb Wataghin - UNICAMP, C.P. 6165, 13083-970 Campinas - SP, Brazil*

(October 26, 2018)

We investigate the role of orbital degeneracy in the double exchange (DE) model. In the $J_H \rightarrow \infty$ limit, an effective generalized “Hubbard” model incorporating orbital pseudospin degrees of freedom is derived. The model possesses an exact solution in one- and in infinite dimensions. In 1D, the metallic phase off “half-filling” is a Luttinger liquid with pseudospin-charge separation. Using the $d = \infty$ solution for our effective model, we show how many experimental observations for the well-doped ($x \simeq 0.3$) three-dimensional manganites $La_{1-x}Sr_xMnO_3$ can be qualitatively explained by invoking the role of orbital degeneracy in the DE model.

PACS numbers: 71.28+d,71.30+h,72.10-d

Colossal magnetoresistance (CMR) materials are presently the focus of much experimental and theoretical attention¹. These materials are important technologically, owing to the huge decrease of resistivity in modest external magnetic fields ($\Delta R/R \simeq 100000$).

Early studies of the models for manganites² concentrated on the observed link between magnetic and transport properties and studied the “double exchange” (DE) model. This simple model certainly has had a surprising degree of success in explaining the existence of the low- T ferromagnetic metallic (FM) phase in doped $La_{1-x}Sr_xMnO_3$ with $x = 0.3$. However, it has come to be subsequently realized that several features of even the high- T phase at $x = 0.3$, not to mention the existence of a very rich phase diagram³, are inexplicable within the framework of the pure DE model. The insulating “normal” state above T_c^{FM} at $x = 0.33$ points to the existence of additional localizing mechanism/s; various candidates considered are (1) a strong coupling of carriers to phonon degrees of freedom⁴, (2) FM short-range order and/or Berry phase effects in the DE model, leading to fluctuations in the hopping and to carrier localization for sufficiently strong spin disorder⁵. The phase diagram of $La_{1-x}Ca_xMnO_3$ is very rich with regions of ferromagnetic, antiferromagnetic and charge order as a function of x ¹. Optical conductivity measurements and photoemission studies⁶ have revealed the transfer of spectral weight over large energy scales, a characteristic of strongly correlated systems. In addition, these studies indicate a small discontinuity in the momentum space occupation fn. $n(\mathbf{k})$, showing up the strongly correlated nature of the FM metallic state. However, the low- T electronic specific heat shows only a modest enhancement of about 2-3 times the bandstructure value⁷. The dc resistivity below T_c^{FM} follows $\rho(T) = \rho_0 + AT^2 + BT^{9/2}$; the first and the last terms can be reconciled with the DE model⁷, but the AT^2 term with a large A decreasing in an applied field, cannot. Recently, Simpson *et al.*⁸ have carried out a careful study of the optical response of $La_{0.7}A_{0.3}MnO_3$ ($A = \text{Ca, Sr}$) crystals, which are ferromagnetic metals at low- T . In contrast with earlier measurements yielding optical masses very different

from those extracted from specific heat data, these authors have found that the effective mass is similarly enhanced in both cases (it is shown⁸ that the differences reported earlier were artifacts of surface effects). Moreover, they extract the scattering rate from their data: the result is $\tau^{-1}(\omega) \simeq -C - D\omega^2$, completely consistent with the quadratic T -dependent component in the resistivity. Raman scattering experiments reveal more confirmation of the importance of electronic correlations below T_c^{FM} ⁸; above T_c^{FM} , the lineshapes can be fit nicely with a constant, large damping, but below T_c^{FM} , good fits can only be obtained by assuming a frequency dependent $\Gamma(\omega) = \Gamma_0 + \alpha\omega^2$, with α increasing with decreasing T , in full accord with the decrease of the dc resistivity. Raman results probing the field dependence of the scattering rate from different channels also shows that the magnetoresistance correlates well with the change in the scattering rate in the B_{1g} channel in an applied field, but that the A_{1g} scattering rate is almost independent of B_{ext} , suggesting an anisotropic scattering rate. Finally, the dc Hall data is very anomalous and defies an explanation,⁹ the normal part implying a large Fermi surface right up to the insulator-metal phase boundary, and the anomalous Hall constant scaling like $[M(0) - M(T)]^{3/2}$ instead of $[M(0) - M(T)]^3$ as expected from a DE model. The above-mentioned facts force one to conclude the existence of an additional scattering mechanism inducing a new low energy coherence scale in the FM metallic state.

The important role of carrier lattice interactions is demonstrated clearly by the isotope effect in T_c^{FM10} , which changes by 20K on substitution of O^{18} by O^{16} ; such behavior requires a consideration of *dynamical* hole-lattice interactions (it is absent in the static limit). Also important in this context are experiments which reveal small polaron transport in the high- T paramagnetic insulating regime (at $x = 0.3$)¹¹. Since T_c^{FM} in the strong coupling limit of the DE model scales with the fermion bandwidth, an electronic bandwidth renormalized by carrier-phonon interaction might be expected to show up the isotope effect in T_c^{FM} .

The regime of charge ordering is more or less unexplored, but seems to be quite anomalous. Recent exper-

imental work has underscored the strong correlation between the magnetic, orbital and lattice degrees of freedom in the manganites. In $La_{1-x}Sr_xMnO_3$, with $x = 1/8$, charge-orbital ordering (COO) was observed by x-ray and neutron diffraction¹², close to commensurate filling fraction of the carriers. This is accompanied by a reentrant transition to an insulating state. Intriguingly, this COO state is *stabilized* by an applied magnetic field B_{ext} , in contradiction to what the pure DE model would suggest. This is because, in the pure DE picture, an external magnetic field would align the core spins, increase the carrier kinetic energy, and *weaken* the COO state. As mentioned in¹², this means that the COO insulating state at low- T is more fully magnetized than the FM-metallic state. In contrast to this, the charge order arising in the $Nd_{0.5}Sr_{0.5}MnO_3$ samples (which are antiferromagnetically ordered) is weakened by applied fields, suggesting a deep connection between magnetic and orbital degrees of freedom that cannot be accessed within the pure DE model.

Clearly, in view of the above anomalous features, effects of orbital degeneracy and carrier-lattice interactions should be considered in a model hamiltonian within a framework which treats their interplay with the magnetic degrees of freedom on an equal footing.

In this paper, we address the issue of the interplay between the magnetic and orbital degrees of freedom. The problem has been a subject of investigation for many years, beginning with the Kugel-Khomskii¹³ paper. In recent years, it has become clear that these effects are crucial for a proper understanding of doped transition metal (TM) oxides¹⁴. However, the full range of new interesting effects has by no means been accessed, and investigation on the role of orbital degeneracy in correlated systems is an active, open problem.

We start with a model that explicitly includes the effects of orbital degeneracy in the e_g orbitals in manganites¹⁵,

$$\begin{aligned}
H = & -t_1 \sum_{\langle ij \rangle} (a_{i\sigma}^\dagger a_{j\sigma} + b_{i\sigma}^\dagger b_{j\sigma} + h.c.) - t_2 \sum_{\langle ij \rangle} (a_{i\sigma}^\dagger b_{j\sigma} + h.c.) \\
& + U \sum_i (n_{ia\uparrow} n_{ia\downarrow} + n_{ib\uparrow} n_{ib\downarrow}) + U_{ab} \sum_{i\sigma\sigma'} n_{ia\sigma} n_{ib\sigma'} \\
& - J_H \sum_{i\sigma\sigma'} \mathbf{S}_i^c \cdot \sigma_i (a_{i\sigma}^\dagger a_{i\sigma'} + b_{i\sigma}^\dagger b_{i\sigma'}) + H_{J-T}, \quad (1)
\end{aligned}$$

where the a and b describe fermion annihilation operators in the doubly degenerate e_g orbitals, U_{ab} is the on-site, interorbital repulsion, U is the on-site, intraatomic Hubbard interaction, and J_H is the (strong) Hund's rule coupling giving rise to the FM state as in the usual DE model. We have also included the polaronic effects via H_{J-T} , as described later in the following. It should be mentioned that the structure of the hopping matrix elements corresponding to the realistic 3d perovskite structure is more complicated than what we have assumed in the model above. This should be crucial when one attempts to focus on the various observed orbitally ordered

(with ferro- or antiferromagnetic order) phases in the global phase diagram. However, in the orbitally disordered ferromagnetic metal phase occurring around $x = 0.3$ that we are interested in here, we believe that a simplified modelling of the hopping matrix suffices, and a more realistic choice will not qualitatively affect our conclusions. In this context, we would like to mention that a similar simplification has been assumed in¹⁵ in a slightly different context. Our main aim here is to demonstrate that orbital correlations, along with double exchange, play a key role in the unified understanding of the various anomalies observed in the FM state around $x = 0.3$.

In the usual DE limit, we are in the regime of $U, J_H \gg t_{1,2}$. This means that the carrier states having their spin antiparallel to the core spin are projected out (we treat the core t_{2g} spin classically, following Furukawa), and so one is effectively dealing with spinless fermions, but with one important difference; the fermions still carry an orbital index. The usual DE model does not include these orbital degrees of freedom, and so cannot access the interplay between magnetism and orbital ordering shown up in manganites. We will show below how inclusion of orbital effects leads to new physics in the manganites, and how many intriguing observations have a natural explanation within our picture.

In the DE limit, the effective hamiltonian is the same as eqn. (1) without the spin index,

$$\begin{aligned}
H = & -t_1 \sum_{\langle ij \rangle} \gamma_{ij}(\mathbf{S}) (a_i^\dagger a_j + b_i^\dagger b_j) \\
& - t_2 \sum_{\langle ij \rangle} \gamma_{ij}(\mathbf{S}) (a_i^\dagger b_j + h.c.) + U_{ab} \sum_i n_{ia} n_{ib}, \quad (2)
\end{aligned}$$

where $\gamma_{ij}(\mathbf{S}) = \frac{\langle S_c \rangle_{ij+1/2}}{2S+1}$ ⁵ is the usual DE factor which describes the fact that the e_g holes increase their kinetic energy by forcing the core t_{2g} spins to align ferromagnetically. At temperatures above the ferromagnetic T_c^{FM} , the FM short range order would imply an effective model with hopping disorder. Varma and Müller-Hartmann *et al*⁶ have proposed that a sufficiently strong hopping disorder could lead to localization of carriers above T_c^{FM} ; such ideas have, however, been challenged by Millis *et al*⁴, who argue for localization caused by strong JT effects at $x = 0.3$. However, no orbital (JT) order is observed at $x = 0.3$ in the FM metallic state (the metallic state is a para-orbital Fermi liquid), leaving one to have to deal with coupled magnetic and orbital degrees of freedom.

Transforming to new pseudo-spin variables, $c_\uparrow = (a + b)/\sqrt{2}$, $c_\downarrow = (a - b)/\sqrt{2}$ yields a generalized Hubbard model with pseudospin-dependent hoppings,

$$\begin{aligned}
H_{eff} = & -(t_1 + t_2) \sum_{\langle ij \rangle} \gamma_{ij}(\mathbf{S}) (c_{i\uparrow}^\dagger c_{j\downarrow} + h.c.) \\
& - (t_1 - t_2) \sum_{\langle ij \rangle} \gamma_{ij}(\mathbf{S}) (c_{i\downarrow}^\dagger c_{j\downarrow} + h.c.) + V \sum_i n_{i\uparrow} n_{i\downarrow}, \quad (3)
\end{aligned}$$

where we call $U_{ab} = V$. In the translationally invariant FM metallic state, $\gamma_{ij}(\mathbf{S}) = \gamma(M)$ where $M = \langle S_i^z \rangle$

is the average core-spin magnetization. Redefining $(t_1 + t_2)\gamma(M) = t_\uparrow(M)$ and $(t_1 - t_2)\gamma(M) = t_\downarrow(M)$, we have finally,

$$H_{eff} = -t_\uparrow(M) \sum_{\langle ij \rangle} (c_{i\uparrow}^\dagger c_{j\uparrow} + h.c.) - t_\downarrow(M) \sum_{\langle ij \rangle} (c_{i\downarrow}^\dagger c_{j\downarrow} + h.c.) + V \sum_i n_{i\uparrow} n_{i\downarrow}. \quad (4)$$

This describes an effective Hubbard-like model with magnetization dependent hopping in *orbital* space. This reflects the correlation between the magnetic and orbital degrees of freedom that we are interested in here. In contrast to the usual one-band Hubbard model, the hamiltonian eqn. (4) has a global symmetry $Z(2) \times U(1)$ in orbital space (it is mapped onto an effective XXZ pseudospin model when $V \gg t$, see below). As we will show in what follows, the effective model, eqn. (4) leads to a more interesting phase diagram than the one obtained from the usual one-band Hubbard model.

In the strong coupling limit, $t\gamma(M) \ll V$, eqn. (4) is mapped to an effective anisotropic pseudo-spin hamiltonian,

$$H_{eff} = 4 \frac{(t_1 + t_2)^2 \gamma^2(M)}{V} \sum_{\langle ij \rangle} \tau_i^z \tau_j^z + 4 \frac{(t_1^2 - t_2^2) \gamma^2(M)}{V} \sum_{\langle ij \rangle} (\tau_i^x \tau_j^x + \tau_i^y \tau_j^y) \quad (5)$$

Our analysis below will be based both on eqs. (4) and (5). To start with, we note the following features which have been exhaustively studied by many workers.¹⁶

(1) $t_1 = t_2$ in eqn. (1). One observes from eqs. (1)-(5) that the “antisymmetric” orbital contribution ($a - b$) decouples from the problem, but interacts with the “symmetric” fermion modes via a local coupling V . In this limit, eqn. (5) becomes a pure Ising model. Eqn. (4) reduces to the well-studied Falicov-Kimball model¹⁶. This has already been employed in connection with the anomalous metallic state in the FM manganites¹⁵. In this situation, the physics, both at and off “half-filling”, has been clear both in one- and in infinite dimensions¹⁶. In 1D, the ground state is characterized by staggered orbital order at $T = 0$, and at a finite $T = T_c > 0$ in $D > 1$. In $d = \infty$, the ground state is charge-ordered, while the paramagnetic metallic phase is a non-Fermi liquid, and is mapped onto the x-ray edge problem. In this case, the spectral fn. of the antisymmetric orbital mode, as well as the mixed orbital excitonic response fn, is singular at $T = 0$ ¹⁶:

$$Im G_{loc}^\downarrow(\omega) \simeq |\omega|^{-(1-\alpha)} \quad (6)$$

and

$$\chi''(\omega) = \int_0^\infty d\tau e^{i\omega\tau} \langle T_\tau c_{\downarrow}^\dagger c_{\uparrow}(\tau); c_{\downarrow}^\dagger c_{\downarrow}(0) \rangle \simeq |\omega|^{-\beta}, \quad (7)$$

where $\alpha = (\delta/\pi)^2$, $\beta = (2\delta/\pi) - (\delta/\pi)^2$, with $\delta = \tan^{-1}(V/D)$ and D the free bandwidth (with $V = 0$). Thus, this non-FL metallic phase is related to the occurrence of a soft, local orbital excitonic mode in our approach.

The breakdown of FLT is caused by a ground state degeneracy $[n_{i\downarrow}, H_{eff}] = 0$ for all i . The exact $d = \infty$ solution shows also that the n_\downarrow varies discontinuously as a function of filling near “half-filling”¹⁶, leading to orbital phase separation. In our case, this corresponds to hole-rich regions (ferromagnetic by the underlying DE mechanism in H_{eff} , with Mn^{4+} , which is JT-inactive), coexisting with the hole-poor (Mn^{3+} , which is JT-active, with underlying AF coming from the remnant of the $x = 0$ insulating state) regions. In this situation, the free energy of the model has a double minimum structure with $n_\downarrow = 0, 1$, leading to low energy multiparticle excitations and an incoherent ferromagnetic metal. Given a non-FL metal, the consequences of static disorder, intrinsic or otherwise, are drastic.

(2) $t_2 = 0$ in eqn. (1). The “two-band” model, eqn. (1), reduces to the usual Hubbard model (in orbital space). This model has an exact solution in 1D, as is known from the Lieb-Wu solution. Away from “half-filling”, it is a non-FL metal with pseudospin-charge separation at low energy¹⁷. Due to the Mermin-Wagner theorem, finite temperature order is ruled out, but it is widely believed that the 2d version has an orbitally ordered ground state. Much more is known in $d = \infty$ ¹⁶. The ground state, at and near “half-filling”, is (in our model) charge ordered. The quantum para-orbital metallic phase obtained by suppressing the low- T ordered state is a correlated Fermi liquid, with a dynamically generated low-energy coherence scale (related to orbital Kondo screening in our model¹⁶) which vanishes as the Mott insulating state (the orbital Mott insulator in our model) is approached by $n \rightarrow 1$ or by $V > V_c$ at $n = 1$.

The most interesting situation, probably the one actually realized in practice, is the one where $t_1 \neq t_2$. Given the actual hopping parameters as in²¹, neither of the cases $t_1 = t_2$ or $t_2 = 0$ is realistic. In this situation, let us consider the physical picture one would expect in $d = \infty$ (which is what we use as an approximation for the 3d manganites). In $d = \infty$, the lattice model is mapped on to a single-impurity Anderson model supplemented with a selfconsistency condition which describes the coupling of the arbitrarily chosen (for a translationally invariant case) “impurity” site to the rest of the lattice. At sufficiently high- T , the orbital moments are unquenched, and the physics is effectively the same as that known from the high- T limit of the usual $d = \infty$ Hubbard model. However, since $t_\downarrow(M)$ can take on arbitrarily small values as $t_1 - t_2$ is varied, the effective low energy coherence scale can be driven quite low, and, in fact, in practice, can be overshadowed by residual disorder effects in doped samples. In the regime where this is true, one is dealing with a two-component picture, with additional strong scattering provided by the orbital moments for $T > T_K^{orb}$. This

additional incoherent scattering mechanism disappears at T_K^{orb} , below which the orbital moments are quenched, leading to a coherent FL response. The difference from the usual situation as encountered in the one-band Hubbard model is that the core-spin thermal fluctuations and two-spinwave processes also contribute. One expects the transport properties to be additive with respect to scattering from orbital and spin fluctuations. As we will discuss below, aspects of the resistivity below T_c^{FM} are naturally understandable in this picture. One would expect disorder or a modest magnetic field to cause dramatic changes in transport properties in this situation because the effective carrier bandwidth has already been narrowed down by orbital correlations, even in the para-orbital phase. At sufficiently low- T , there is an instability to an orbital-ordered state when the filling is close to commensurate values, in analogy with what is known about the Hubbard model in this limit.

We turn now to the effects of adding polaronic term via strong Jahn-Teller coupling in the above formalism. The modelling essentially duplicates that employed by Millis *et al*⁴; here, the local lattice distortions which cause the Jahn-Teller splitting transform as a two-fold degenerate representation of the cubic group which couple to the electron as a traceless symmetric matrix. The JT part is

$$H_{J-T} = \lambda \sum_i (Q_{2i}\tau_i^z + Q_{3i}\tau_i^x) + K/2 \sum_i (Q_{2i}^2 + Q_{3i}^2) + M_0/2 \sum_i [(dQ_{2i}/dt)^2 + (dQ_{3i}/dt)^2], \quad (8)$$

where $Q_2 = (2\delta Z - \delta X - \delta Y)/6^{1/2}$ and $Q_3 = (\delta X - \delta Y)/2^{1/2}$, where λ is the electron-phonon coupling, K is the phonon stiffness, and M_0 the ionic mass. We can define⁴ the distortion vector \mathbf{Q} by $Q_x = Q_3$ and $Q_z = Q_2$, so that $H_{JT} = \lambda \sum_i \mathbf{Q}_i \cdot \boldsymbol{\tau}_i$. Further, we consider a fixed $|\mathbf{Q}|$, so that the distortions are modeled by a local classical spin. In the adiabatic limit for the phonons, and for strong coupling, the JT part acts like additional double exchange. As T increases, fluctuations in the Q_i become important.

Thus, an enormous simplification occurs: the original two-band model is mapped onto a generalized orbital Hubbard model with magnetization dependent hoppings with an additional ‘‘double exchange’’ coming from the JT term. The effective hamiltonian is

$$H_{eff} = -t_\uparrow(M) \sum_{\langle ij \rangle} (c_{i\uparrow}^\dagger c_{j\uparrow} + h.c) - t_\downarrow(M) \sum_{\langle ij \rangle} (c_{i\downarrow}^\dagger c_{j\downarrow} + h.c) + V \sum_i n_{i\uparrow} n_{i\downarrow} - g \sum_i \tau_i \cdot \mathbf{Q}_i + k/2 \sum_i Q_i^2, \quad (9)$$

with $t_\alpha(M) = t_\alpha[(1 + M^2)/2]^{1/2}$. In addition, interactions between lattice distortions at different sites is will stabilize a particular distortion direction. We model this effect by introducing a term $h' = \kappa \sum_{\langle ij \rangle} Q_i^\alpha Q_j^\alpha$ with κ chosen to be ferromagnetic⁴. This is consistent with the

observation in the FM metallic state, and consideration of staggered phases will require a two-sublattice extension. We do not consider this in this work.

To simplify matters further, it is convenient to introduce a local pseudospin quantization axis parallel to the local \mathbf{Q}_i at each site. This rotation from a fixed quantization axis to the local one corresponds to diagonalizing the JT part above by a local unitary transformation, U_i : $U_i^\dagger[(\boldsymbol{\tau}_i \cdot \mathbf{Q}_i)/Q_i]U_i = \tau_{iz}$. One has simultaneously to transform the electron operators as, $a_{i\sigma} = U_i c_{i\sigma}$. After doing the transformations, the effective hamiltonian takes the form,

$$H_{eff} = \sum_{\langle ij \rangle, \sigma, \sigma'} t_{ij}(\mathbf{S}) U_i^\dagger U_j a_{i\sigma}^\dagger a_{j\sigma'} + V \sum_i n_{i\uparrow} n_{i\downarrow} - g \sum_{i\sigma} Q_i \sigma n_{i\sigma} + k/2 \sum_i Q_i^2. \quad (10)$$

Notice that the JT term has been rendered simpler, but we have to pay the price by having to consider a complicated hopping term. However, in the FM state around $x = 0.3$, there is no orbital LRO, and at low- T , there is no evidence for localization effects. The off-diagonal dependence of t_{ij} is then not crucial in this regime, and so we replace $U_i^\dagger t_{ij} U_j = t_{eff}$. With this assumption, we have reduced our problem to that of a Hubbard model in orbital space, with an additional site-diagonal (random in the para-orbital state ($x = 0.3$) ‘‘disorder’’ potential coming from the disordered (or short-range-ordered) JT distortions. This term acts like a random magnetic field on the orbital pseudospins. Given this, the effective hamiltonian is solved within $d = \infty$ by *iterated perturbation theory*, extended to include effects arising from repeated scattering due to diagonal disorder¹⁸. In what follows, we will use the extended IPT (IPT+CPA) to treat the combined effects of orbital (Hubbard-like) correlations and static (JT) disorder in the low- T ferromagnetic metallic state around $x = 0.3$.

We use the $d = \infty$ solution¹⁶ of the Hubbard-like model without the JT-term (since no JT distortion is observed in the FM state at $x = 0.3$) to provide a simple understanding of various features observed in experiments. Firstly, we notice that the anomalous stabilization of the CO state in external magnetic fields has a simple explanation: B_{ext} increases the effective hopping in the above eqn., leading to an increase in T_{CO} , via $T_{CO} \simeq (t^2 \gamma^2(M)/V)$ for $V \gg t$ (since the orbital AF state is the analog of the Neel-ordered AF state in the usual Hubbard model) as can be seen from the Hubbard model physics in $d = \infty$ on simple cubic lattice both in the weak and strong coupling regimes. If this low- T transition is indeed driven by the development of orbital ordering, via the above mechanism, T_{CO} should show an isotope effect, which we quantify later. Clearly, this requires the orbital effects via V , and so arises from the correlation between orbital and magnetic degrees of freedom, as envisaged in¹². In the ‘‘overdoped’’ samples ($x = 0.33$), one is in the ‘‘weak scattering’’ regime, with a

Fermi liquid response at low- T . The transfer of spectral weight with T , a characteristic feature of manganites, again has a natural interpretation in terms of Hubbard model physics with magnetization dependent hoppings, as in the above eqn.

Quite generally, the optical conductivity in $d = \infty$ is given by a simple bubble diagram involving the full $d = \infty$ local GF $G_{loc}(i\omega_n)$:¹⁶

$$\sigma(\omega) = \frac{2e^2 t_{\uparrow}^2(M) a^2}{\Omega \hbar^2} \int_{-\infty}^{\infty} dE D(E) \int_{-\infty}^{\infty} \frac{d\omega'}{2\pi} \langle \rho(E, \omega') \rangle \times \langle \rho(E, \omega + \omega') \rangle \frac{n_F(\omega') - n_F(\omega' + \omega)}{\omega}, \quad (11)$$

where $\langle \rho(E, \omega) \rangle = -Im \langle [\omega - E - \Sigma(\omega)]^{-1} \rangle / \pi$ is the disorder-averaged single-particle spectral fn. of the disordered Hubbard model.

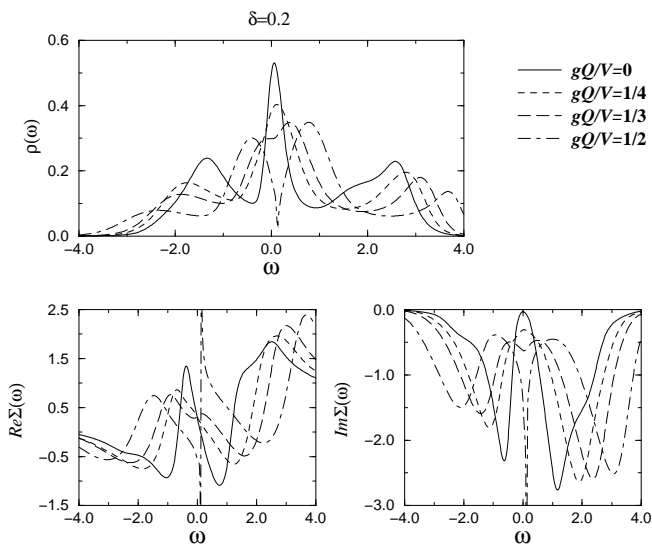


FIG. 1. Local spectral density and the real and imaginary parts of the s.p self energy for the disordered, orbital Hubbard model in the paper in $d = \infty$ at $T = 0.01D$. Notice the sharp FL feature without JT disorder, which is broadened out for small Q_i while preserving the FL picture (dashed line). This corresponds to the FM metallic phase of the manganites. With increasing Q_i , a pseudogap opens up in $\rho(\omega)$, and the scattering rate describes an incoherent non-FL metal.

In fig. (1), we show the density of states and the self-energy for the model in $d = \infty$. We choose $x = n = 0.8$, $U/D = 3.0$ and $\lambda/D = 0.2$. These parameters are realistic if D is chosen to be around $1eV$. We also choose a simple binary distribution for the JT disorder; this is motivated by the fact that the Mn^{4+} octahedra are JT-undistorted- only the Mn^{3+} are JT-distorted. This effective disorder is modelled by $P(Q_i) = (1 - x)\delta(Q_i) + x\delta(Q_i - Q)$. We restrict ourselves to the low- T state, and so choose $T = 0.01D$. Notice that $Im\Sigma(\omega) \simeq -C - D\omega^2$, in good accord with the results extracted from the optical data of Simpson *et al*.⁸. The carrier scattering rate thus goes quadratically with ω, T , as seems to be observed in

the FM metallic state. Simultaneously, $Re\Sigma(\omega) \simeq -a\omega$ at low energy, and the quasiparticle picture is valid in spite of JT disorder. For comparison, we also show the results without disorder; in this case, our results are in good agreement with those from earlier studies¹⁶; this serves as a check on our numerics. The longitudinal optical conductivity, computed using the above eqn, also reveal features in good agreement with those observed in experiments. As T is lowered, the FM spin polarization increases, leading to increase in $t_{1,2}$ and, within Hubbard model physics in $d = \infty$, to a transfer of spectral weight on a scale of V from the high-energy incoherent part to a low energy quasicohherent peak. Furthermore, the optical conductivity experiments reveal that the low energy spectral weight scales like $\gamma^2(M) = (1 + M^2)/2$ at low- T (but not above T_c^{FM}), exactly as is expected from the effective hamiltonian above. In the low- T FM metallic phase, we see clearly the Drude response at low energy, followed by a broad hump at higher energy; we attribute this to the orbital correlations in the e_g sector (U) in the model above. Notice that in presence of strong orbital correlations, the spectral weight transfer from high to low energies is controlled by the ratio $V/t_{ab}(M)$ (which is T -dependent in our model, via the T -dependence of M); as T decreases, $M(T)$ and hence $t_{ab}(M)$ increases, reducing the ratio $V/t_{ab}(M)$ and leading to a transfer of spectral weight from high- to low energies, as observed. While the spectral weight transfer with T can be rationalized by simple DE models², the small weight of the quasicohherent Drude peak⁸, as well as the intense mid-infrared absorption is clearly unexplainable in such approaches, but has a natural interpretation within our picture, where it arises from the transition from the “lower Hubbard subband” (in the doubly degenerate e_g sector) to the quasicohherent Kondo like peak, as in the usual Hubbard model in $d = \infty$ ¹⁶.

Fig.(2) indeed shows these features; the JT “disorder” broadens the Drude peak somewhat, yielding the constant C in the scattering rate, while leaving the ω^2 part unchanged. The mid-IR peak, corresponding to transitions between the lower-Hubbard band and the quasiparticle resonance in the $d = \infty$ Hubbard model, is shifted somewhat, to $\omega' = V/2 + gQ$, and the high-energy feature (completely broadened out) corresponds to transitions between the Hubbard bands. Our computed result for the optical conductivity with $gQ/V = 1/4$ is in good agreement with the thin film results of Simpson *et al*.⁸. With increasing gQ/V (fig.2), we see that the optical response at low energies is totally incoherent, as was indeed observed in earlier studies⁶. In our picture, this is simply a consequence of the increased strong scattering from JT- as well as doping induced disorder, which produces an incoherent spectral density and a non-Drude optical response. The s.p scattering rate is related to $Im\Sigma(\omega) \simeq -(V^2/D_{\uparrow}^2 D_{\downarrow})\omega^2 n_{\downarrow}(1 - n_{\downarrow})$, within second-order perturbation theory (this actually gives the correct FL estimate at low energy in $d = \infty$). This implies a real

part that goes like $Re\Sigma(\omega) = -(V^2/D_{\uparrow}^2)n_{\downarrow}(1-n_{\downarrow})\omega$, and

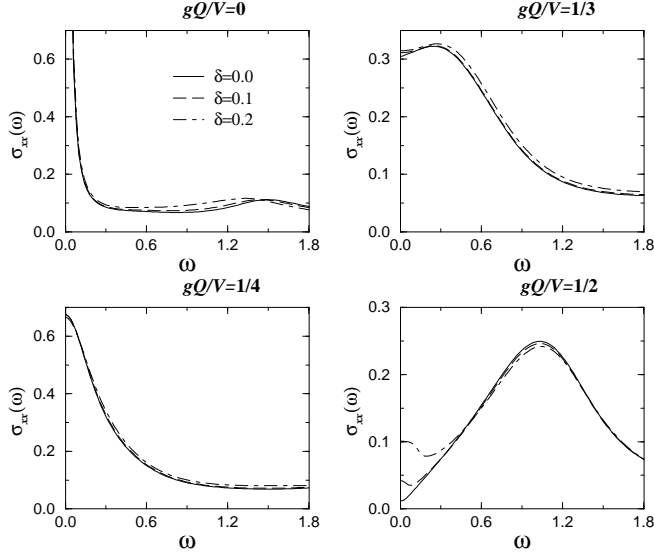


FIG. 2. Optical conductivity, $\sigma_{xx}(\omega)$ of the disordered, orbital Hubbard model in $d = \infty$ as a fn. of doping for various values of the JT disorder, $gQ/V = 0, 1/4, 1/3, 1/2$. The case $gQ/V = 1/4$ corresponds most closely to the conditions of ref.⁸. Notice the somewhat broadened, but still dominant, Drude response at low energy, followed by a mid-IR hump that carries a large fraction of the total optical weight. The other curves may correspond to situations with larger ratio gQ/V , as in situations where small or no Drude response is seen.

hence the quasiparticle residue at μ is $Z = (1 + (V/D)^2 n_{\downarrow}(1 - n_{\downarrow}))^{-1}$. So $m^*/m \simeq 3$ for $V = 3D$ and $x = 0.3$, giving a specific heat enhancement in the observed range. Notice that this is also close to the optical mass extracted by Simpson *et al.* from their optical measurements, confirming that charge (orbital) ordering tendencies are not important deep in the FM metallic state. The above calculation also shows that the resistivity, $\rho(T) \simeq AT^2$ with $A = (V^2/D_{\uparrow}^2(M)D_{\downarrow}(M))$ decreasing with increasing B_{ext} , as observed. The other terms correspond to elastic scattering off the core-spin and the inelastic scattering off two-magnon fluctuations, and are given by $\rho_m(T) \simeq \rho_0 + BT^{9/2}$ as shown by Kubo. Since the scattering off spin as well as orbital fluctuations correspond to single-site processes in $d = \infty$, it follows that the total scattering rate is the sum of those coming from magnetic and orbital scattering. This gives a consistent explanation of $\rho(T)$ below T_c^{FM} . More importantly, it is also consistent with results from Raman scattering experiments, as seen from the following argument. In $d = \infty$, the vertex corrections do not enter the conductivity¹⁶; in this approximation the Raman intensity is simply related to the conductivity as long as the incident laser frequency is not close to those corresponding to resonant scattering. The Raman intensity is given by¹⁹,

$$I(\omega) = \frac{\omega}{1 - e^{-\beta\omega}} \sigma'_{xx}(\omega). \quad (12)$$

Using the Drude form for $\sigma_{xx}(\omega)$ in the para-orbital FL regime, $\sigma_{xx}(\omega) = \frac{\omega_p^2/4\pi}{1/\tau - i\omega}$, with $1/\tau \simeq xIm\Sigma(\omega, T) + \Gamma_0$, where Γ_0 is the impurity contribution to the scattering rate (from residual disorder) gives, for $\omega \ll k_B T$,

$$I(\omega) = \frac{\omega_p^2}{4\pi} k_B T \frac{1}{\Gamma_0 + xA(M)\omega^2 - i\omega}, \quad (13)$$

with $\alpha = xA(M) = xV^2/D_{\uparrow}^2(M)D_{\downarrow}(M)$. This explains the coherent $Im\Sigma(\omega) = \Gamma_0 + \alpha\omega^2$ term needed to understand Raman lineshapes below T_c^{FM} . Since the self-energy is purely local in $d = \infty$, the Fermi surface is unchanged (from its bandstructure value) by interactions in the para-orbital metallic state. The discontinuity in $n(\mathbf{k})$, the momentum occupation fn, is reduced by interactions, and is quite small for $V = 3D$ (off $n = 1$)¹⁶, completely consistent with the small discontinuity observed in the FM metallic state at $x = 0.3$. The Fermi surface is large, as expected from bandstructure calculations, and in agreement with the small value of the Hall constant. Notice that calculation of the normal contribution to the Hall coefficient in the $d = \infty$ Hubbard model²⁰ would yield a small value of $R_H(x)$ for $x \simeq 0.3$, consistent with the above. Since the bandwidth D increases in an external magnetic field via $\gamma(M)$, the coefficient A decreases, and we predict enhancement of the linear specific heat coefficient with B_{ext} , as well as a decreased value of R_H , which seem to be observed in the FM metallic state.

The dynamical effects of the JT term can now be considered. At low- T , the effects of electron-lattice interaction can be absorbed into the effective V in our orbital Hubbard model. Given an optical phonon frequency ω_0 , at temperatures $T \ll \hbar\omega_0/k_B$, one can integrate out the phonons, generating a term $H' \simeq \frac{\lambda^2}{\hbar\omega_0} \sum_i [c_{i\alpha}^\dagger(\tau/2)c_{i\beta}]^2$. At low- T , with $J_H \rightarrow \infty$, this looks like an additional Hubbard interaction in orbital space, and so the results obtained above are qualitatively unaffected except for the change $V \rightarrow V + \frac{\lambda^2}{\hbar\omega_0}$. Given a larger V_{eff}/D in our orbital Hubbard model, the consequence within DMFT will be to decrease the coherent spectral weight, moving it to the incoherent, high-energy region. Thus, the A in the quadratic term in the resistivity will be $A = V_{eff}^2/D_{\uparrow}^2 D_{\downarrow}$, and the Drude-like component in the optical conductivity is further suppressed. At higher T , a description involving static JT distortions should suffice⁴. Finally, since $T_c^{FM} \simeq D^* = ZD(\omega_0)$, where $D(\omega_0) = De^{-\lambda^2/\omega_0^2}$ is the polaron reduction of the bandwidth⁴ in the DE model with $J_H \rightarrow \infty$, the scaling of the FM transition temperature with ionic mass is given by

$$k_B T_c^{FM} = \frac{D}{1 + ((V + \lambda^2/\hbar\omega_0)/D)^2 n_{\downarrow}(1 - n_{\downarrow})}, \quad (14)$$

with $\omega_0^2 = K/M_O$. This represents a different way of understanding the isotope effect in T_c^{FM} as arising from

two effects; a polaron induced narrowing of the bandwidth, and a renormalization of the effective V by carrier-phonon interactions. Notice that such an explicit dependence on ω_0 is absent in the adiabatic treatment of the phonons (in agreement with Röder *et al.*⁴).

Finally, the orbital-charge ordering in the $x = 1/8$ sample should show an isotope effect via $k_B T_{CO} \simeq (t^2 \gamma^2(M)/V_{eff})$; i.e, a reduced isotopic mass M will increase ω_0 and decrease V_{eff} thus stabilizing the CO ordered state. We are not aware of experiments addressing this issue, but we point out that it would be a nice confirmation of the importance of (strong) orbital correlations + JT effects in the CMR manganites.

Consideration of the high- T "insulating" phase requires more work; to see this, notice that with strong $gQ > D$, the combined effects of disorder and interactions in H_{eff} will be to localize the carriers. The decrease in the effective bandwidth (via decreasing $\gamma(M)$ above T_c^{FM} favors carrier localization, and the enhancement of D below T_c^{FM} delocalizes the carriers (by moving the effective λ/D ratio through a critical value required for carrier delocalization. An external magnetic field has precisely this effect; the increase of $D(M)$ suppresses the high- T insulating state, leading to the CMR effect. The consideration of localization effects crucial for such a scenario is outside the scope of the $d = \infty$ approach¹⁶, and, indeed, we shall return to this question in a separate work. Consideration of dynamical charge and spin correlations and their effects on magnetotransport near the various charge-orbital ordered phases in the global phase diagram requires a consideration of realistic hopping matrix elements, and more importantly, the inclusion of short-ranged (non-local) dynamical correlations in a proper extension of the DMFT (e.g, via the dynamical cluster approximation (DCA)²¹). We plan to report such studies in a future publication.

To summarize, the low- T features in the well doped FM metallic state of the manganites can be understood in a unified way based on the exact $d = \infty$ solution of the strong coupling ($U, J_H \rightarrow \infty$) double exchange model with inclusion of the orbital degeneracy and Jahn-Teller effects. We have shown that orbital fluctuations play a very important role in the understanding of key features of the dc and ac transport even in the FM metallic state. Specifically, orbital correlations generate a low-energy coherence scale that is sensitive to external magnetic fields. Additionally, these correlations narrow down the bandwidth, making it easier for a combination of hopping and structural disorder to induce carrier localization. Recent work by Held *et al.*²² considers the effect of the orbital U in the paramagnetic phase of the manganites. However, the effects of the disordered Jahn-Teller coupling has not been considered there. In contrast, we have considered these effects along with strong interorbital correlations on the same footing, and have made a somewhat detailed comparison with experimental results in the low- T FM state. Our work is thus complementary to theirs.

Recently, Nagaosa *et al.*²² have shown that a slightly

extended version of the model considered here (including super exchange terms) and realistic hopping matrix elements gives a good agreement with the experimentally observed phase diagram over the whole range of x . We expect our simplified model (neglecting superexchange) to be an adequate starting point to describe the FM metallic state at $x = 0.3$. It can be shown that inclusion of realistic hopping matrix elements will not qualitatively affect the conclusions obtained above in $d = \infty$; they will, however, be crucial when one attempts to understand the phase diagram, which shows a rich sequence of transitions as a function of x . We have not attempted to do this here; a more detailed numerical investigation to consider these additional details is under progress and will be reported separately.

ACKNOWLEDGMENTS

One of us (MSL) acknowledges financial support of SFB 341. LC was supported by the Fundação de Amparo à Pesquisa do Estado de São Paulo (FAPESP) and the Max-Planck Institut für Physik komplexer Systeme.

-
- ¹ see, for example, *Colossal Magnetoresistive Oxides*, ed. Y. Tokura (Gordon and Breach Publishers) in press.
 - ² P. W. Anderson and H. Hasegawa, *Phys. Rev.* **100**, 675 (1955); N. Furukawa, *J. Phys. Soc. Jpn.* **63**, 3214 (1994), *ibid* **64**, 3164 (1995).
 - ³ H. Kuwahara *et al.*, in *Phase Diagram and Anisotropic Transport Properties of Nd_{1-x}Sr_xMnO₃ Crystals*, MRS Symposium, Proc. Number 494, Pittsburgh (1998), p. 83.
 - ⁴ A. J. Millis, P. B. Littlewood and B. Shraiman, *Phys. Rev. Lett.* **74**, 5144 (1995), *Phys. Rev.* **B54**, 5389 (1996); H. Röder *et al.*, *Phys. Rev. Lett.* **76**, 1356 (1996).
 - ⁵ C. M. Varma, *Phys. Rev.* **B54**, 7328 (1996); E. Müller-Hartmann and E. Dagotto, *Phys. Rev.* **B54**, R6819 (1996).
 - ⁶ Y. Okimoto *et al.*, *Phys. Rev. Lett.* **75**, 109 (1995). For photoemission results, see D. Dessau *et al.*, *Phys. Rev. Lett.* **81**, 192 (1998).
 - ⁷ T. Okuda *et al.*, *Phys. Rev.* **B61**, 8009 (2000).
 - ⁸ R. Simpson *et al.*, cond-mat 9908419.
 - ⁹ R. Matl *et al.*, *Phys. Rev.* **B57**, 10248 (1998); see also, W. Westerburg *et al.*, *European Phys. Journal.* **B14**, 3, 509 (2000).
 - ¹⁰ G. Zhao *et al.*, *Nature*, (London)**381**, 676 (1996).
 - ¹¹ see, for example, H. Y. Hwang *et al.*, *Phys. Rev. Lett.* **75**, 914 (1995); P. Schiffer *et al.*, *ibid* **75**, 3336 (1995).
 - ¹² S. Uhlenbruck *et al.*, *Phys. Rev. Lett.* **82**, 185 (1999).
 - ¹³ K. Kugel and D. Khomskii, *Sov. Phys. JETP* **37**, 725 (1973).
 - ¹⁴ T. M. Rice, in *Spectroscopy of Mott Insulators and Correlated Metals*, eds. A. Fujimori and Y. Tokura (Springer, Berlin, 1995).

- ¹⁵ V. Ferrari *et al.*, cond-mat/9906131.
- ¹⁶ see, for example, A. Georges *et al.*, Rev. Mod. Phys. **68**, 13 (1996).
- ¹⁷ *Bosonization and Strongly Correlated Systems*, by A. Tsvelik, A. Nersesyan and A. Gogolin, Cambridge University Press (1998).
- ¹⁸ M. S. Laad, L. Craco and E. Müller-Hartmann, cond-mat/9911378, submitted to Phys. Rev. B.
- ¹⁹ B. S. Shastry and B. I. Shraiman, Phys. Rev. Lett. **65**, 1068 (1990).
- ²⁰ P. Majumdar and H. R. Krishnamurthy, cond-mat/9512151.
- ²¹ H. Hettler *et al.*, Phys. Rev. B **58** R7475 (1998).
- ²² K. Held and D. Vollhardt, cond-mat/9909311, to appear in Phys. Rev. Lett.
- ²³ R. Maezono, S. Ishihara and N. Nagaosa, Phys. Rev. B **58**, 11583 (1998).